NIH Public Access
Author Manuscript
Biochemistry. Author manuscript; available in PMC 2011 May 4.

Published in final edited form as:
Biochemistry. 2010 May 4; 49(17): 3640–3647. doi:10.1021/bi100328j.

Evidence for a Bicarbonate "Escort" Site in *Haemophilus influenzae* β-Carbonic Anhydrase, †,‡

Roger S. Rowlett[*,§], **Katherine M. Hoffmann**[§], **Hannah Failing**[§], **Margaret M. Mysliwiec**[§], and **Dejan Samardzic**[§]

[§]Department of Chemistry, Colgate University, 13 Oak Drive, Hamilton, NY 13346

Abstract

The *Haemophilus influenzae* β-carbonic anhydrase (HICA) allosteric site variants V47A and G41A were overexpressed and purified to homogeneity. These variants have k_{cat}/K_m values similar to wild-type enzyme, and exhibit a similar dramatic decrease in catalytic activity at *p*H values below 8.0. However, both HICA-G41A and -V47A were serendipitously found to bind sulfate ion or bicarbonate ion near pairs of Glu50 and Arg64 residues located on the dimerization interface. In the case of HICA-V47A, bicarbonate ions simultaneously bind to both the dimerization interface and the allosteric sites. For HICA-G41A, 2 of 12 chains in the asymmetric unit bind bicarbonate ion exclusively at the dimerization interface, while the remaining 10 chains bind bicarbonate ion exclusively at the allosteric site. We propose that the new anion binding site along the dimerization interface of HICA is an "escort" site that represents an intermediate along the ingress/egress route of bicarbonate ion to/from the allosteric binding site. The structural evidence for sulfate binding at the "escort" site suggests that the mechanism of sulfate activation of HICA is the result of sulfate ion competing for bicarbonate at the "escort" site, preventing passage of bicarbonate from bulk solution to its allosteric site.

Keywords

beta carbonic anhydrase; *Haemophilus influenzae*; allosteric site; bicarbonate; zinc metalloenzyme

Carbonic anhydrases (carbonate hydrolyase, EC 4.2.1.1, CA[1]) are metalloenzymes that catalyze the interconversion of CO_2 and bicarbonate:

$$CO_2 + H_2O \leftrightarrows HCO_3^- + H^+ \quad (1)$$

†This work was supported in part by a grant (to R.S.R.) from the National Science Foundation (MCB-0741396), and upon research conducted at the Cornell High Energy Synchrotron Source (CHESS), which is supported by the National Science Foundation and the National Institutes of Health/National Institute of General Medical Sciences under NSF award DMR-0225180, using the Macromolecular Diffraction at CHESS (MacCHESS) facility, which is supported by award RR-01646 from the National Institutes of Health, through its National Center for Research Resources.

‡Coordinates and structure factors have been deposited in the Protein Data Bank as entries 3E2X, 3E31, 3E3F, 3E3G, and 3E3I

*To whom correspondence should be addressed; rrowlett@colgate.edu, phone, (315)-228-7245; fax (315)-228-7935.

Supporting Information Available: A figure (S1) depicting the bicarbonate binding site in *M. tuberculosis* mycolic acid cyclopropane synthase CmaA2, which shares key features with the bicarbonate "escort" site in HICA, is included in supporting information. This material is free of charge via the internet at http://pubs.acs.org.

[1]Abbreviations: CA, carbonic anhydrase; HICA, *Haemophilus influenzae* β-carbonic anhydrase; ECCA, Escherichia coli β-carbonic anhydrase; ICP-OES; inductively coupled plasma-optical emission spectroscopy; EDTA, *N*,*N*,*N*′,*N*′-ethylenediaminetetraacetic acid; PCR, polymerase chain reaction; PEG-400, polyethylene glycol 400; HEPES, 4–(2-hydroxyethyl)piperazineethanesulfonic acid

NIH-PA Author Manuscript
NIH-PA Author Manuscript
NIH-PA Author Manuscript

NIH-PA Author Manuscript

NIH-PA Author Manuscript

NIH-PA Author Manuscript

The β-CAs are one of five convergently evolved classes of CA, and are widespread in eubacteria and plants. All β-CAs that have been characterized to date are zinc-metalloenzymes. *Haemophilus influenzae* carbonic anhydrase (HICA) is a "type II" member of the β-carbonic anhydrase family (1). Type II β-CAs are able to adopt a structure in which the catalytically essential zinc-bound water molecule can be displaced by an active site Asp residue. In addition, type II β-CAs have a characteristic triad of non-catalytic residues (Trp39, Arg64, and Tyr181 in HICA) about 8 Å away from the active site zinc ion that can bind bicarbonate ion. For HICA and ECCA, kinetic and structural evidence strongly suggests that this noncatalytic bicarbonate ion is a negative allosteric effector that stabilizes an inactive, T-state conformation of the enzyme, where Asp44 displaces the catalytically essential zinc-bound water (2). The X-ray crystallographic structures of Type I (non-allosteric) β-CAs and the D44N variant of HICA suggest that Type II β-CAs can also adopt an active, R-state conformation in which Asp44 pairs with Arg46, allowing the coordination of the catalytically essential water molecule to the active site zinc ion (3). The noncatalytic bicarbonate ion is believed to stabilize the inactive T state (Scheme 1), and this hypothesis is borne out by the W39F variant of HICA in which bicarbonate ion is significantly less effective in inhibiting the enzyme (3).

A key player in the allosteric (T → R) transition of HICA in Scheme I is Val47: the steric bulk of this side chain is hypothesized to displace bicarbonate from the allosteric binding site in the R state, and thus provides the necessary steric coupling mechanism between the bicarbonate binding and the adopted allosteric state. In addition, examination of X-ray crystallographic structures of type I and type II β-CA reveals that type I β-CAs all have a slightly more bulky Ala41 residue rather than the smaller Gly41 in type II β-CAs. Examination of type II β-CA structures with Gly41 altered to Ala suggests that this structural change may preclude bicarbonate binding to the allosteric site (1). To investigate the roles of these residues we kinetically and structurally characterized the G41A and V47A variants of HICA.

Surprisingly, we find that these variants have little impact on the catalytic function of HICA. However, we have serendipitously discovered that these variants are able to bind bicarbonate ion in an intermediate binding site that apparently defines the entry/exit pathway of bicarbonate to/from the allosteric site. These results suggest that the mechanism of allosteric inhibition of HICA, and the selectivity of the allosteric binding site is more complex than previously recognized.

Experimental Procedures

Expression and purification of wild-type and recombinant enzymes

Wild type HICA was prepared as previously described (2). Site-directed mutations of the gene coding for HICA were constructed using megaprimer PCR (4) with *Vent* (New England Biolabs) or *Pfu* turbo (Stratagene) polymerase and commercial oligonucleotides (Integrated DNA Techonolgies). For variant V47A, a mutated oligonucleotide[2] 5′-TTCAGCAGGC**CGC**ACGGCTATC-3′ was paired with the 5′ oligonucleotide primer PHI1X (5′-TGCCCATGGATAAAATTAAACAACTCTTT-3) in the first PCR reaction to give a 129 bp product. This PCR product was used as a megaprimer in a second PCR reaction with the 3′ oligonucleotide primer PHI2X (5′-TGCCTGCAGTTATTATGTATTTTCAAGATG-3′) to create the final mutated HICA gene. The final PCR product was digested with *Nco*I and *Pst*I (Promega) and ligated (Quick Ligase, New England Biolabs) into pTrc99a vector digested with the same enzymes. Variant G41A was constructed similarly using the mutated oligonucleotide 5′-ATCAGAGCA**AGC**AATCCAAAG-3′. All expression plasmids were subjected to DNA

[2]Mutation site of oligonucleotides are bolded; restriction endonuclease sites for cloning are underlined.

NIH-PA Author Manuscript

NIH-PA Author Manuscript

NIH-PA Author Manuscript

sequencing (PE Biosystems ABI 310, BigDye 3.0 chemistry) of the entire HICA gene to verify introduction of the correct mutation.

Expression, purification, storage, and quantification of variant HICA proteins was exactly as described for the wild-type protein (2). Briefly, crude homogenates of overexpressed protein were purified to homogeneity by ion exchange (Q-Sepharose FF), hydrophobic interaction (butylsepharose FF), and gel exclusion chromatography (Superdex 200) using an AKTA FPLC (GE Healthcare), and quantified by ICP-OES (Perkin Elmer Optima SC 3000) for zinc at 213.856 nm.

Steady-State Kinetics Methods

Saturated solutions of CO_2 were prepared by bubbling CO_2 gas into water in a vessel maintained at 25.0 ± 0.1 °C, and dilutions prepared in the absence of air by coupling two gas-tight syringes as described by Khalifah (5). CO_2 concentrations were calculated based on a 33.8 mM saturated solution at 25 °C (6).

All steady state kinetic measurements were made at 25 °C using a Hi-Tech SF-61DX2 stopped-flow spectrophotometer. Initial rates of CO_2 hydration were measured using the changing pH-indicator method described previously (5,7,8). All stopped-flow kinetic studies were carried out in the presence of 250 mM Na_2SO_4, which was required for maximum enzyme stability and activity in dilute solution (2). Values of k_{cat} and K_m were determined by non-linear least squares fits to v/[E] *vs.* [CO_2] data using Origin 7.0 (Microcal). For all kinetics measurements reported here, substrate dependence of CO_2 hydration rates appeared to follow Michaelis-Menten kinetics. The kinetic constants k_{cat} and k_{cat}/K_m are reported here on a per subunit basis.

Crystallographic methods

Starlike clusters of orthorhombic plates of HICA-V47A appeared after 3 months in 1.7 M ammonium sulfate, 4% PEG 400, 0.10 M HEPES pH 7.50, 6 mg/mL protein at 4 °C using hanging drop vapor diffusion. Crystals were soaked in artificial mother liquor plus 30% glucose for 30-60 seconds prior to flash cooling in liquid nitrogen. Data collection for PDB 3E2X was carried out at beamline F2 of CHESS at a wavelength of 0.98 Å detector using 0.5° oscillations at a temperature of 100 K.

Tetragonal crystals of HICA-V47A were grown in 2-3 days in 0.7 M sodium potassium tartrate, 0.10 M HEPES, pH 7.50, 12 mg/mL protein at 22 °C. Crystals were soaked for 1-2 minutes in artificial mother liquor plus either 30% glucose (PDB 3E31) or 30% glucose and 100 mM $NaHCO_3$ (PDB 3E3F) before flash cooling in liquid nitrogen. Data collection was carried out at beamline F2 of CHESS at a wavelength of 0.98 Å detector using 0.5° oscillations at a temperature of 100 K.

Monoclinic crystals of HICA-G41A were grown in 2-3 days in 1.8 M ammonium sulfate, 4% PEG-400, 0.10 M HEPES, pH 7.50 12 mg/mL protein at 22 °C. Crystals were soaked for 1-2 minutes in artificial mother liquor plus either 30% glucose (PDB 3E3G) or 30% glucose and 100 mM $NaHCO_3$ (PDB 3E3I) before flash cooling in liquid nitrogen. Data collection was carried out at beamline F2 of CHESS at a wavelength of 0.98 Å detector using 0.5° oscillations at a temperature of 100 K.

Data was processed using MOSFLM (9) and SCALA (10), and an initial molecular replacement solution as obtained by using a search model using a single dimer (HICA-V47A) or three tetramers (HICA-G41A) of wild-type HICA (PDB 2A8D) in Phaser (11). The initial solution was subjected to multiple rounds of refinement using Refmac5 (12) and model-building in Coot (13). Final refinement used TLS (14) with one TLS group per protein chain.

NIH-PA Author Manuscript

NIH-PA Author Manuscript

NIH-PA Author Manuscript

Data collection and refinement statistics are reported in Table 1.

Results

Overexpression and purification of HICA variants V47A and G41A

HICA variants V47A and G41A were overexpressed at levels of ≈15% of total protein in *E. coli*, and were purified to homogeneity using previously established methods for the wild-type enzyme (2). Elution volumes of both HICA-G41A and V47A on a calibrated gel exclusion column (Supedex-200, Amersham) during the final purification step indicated an apparent molecular mass of ≈100 kDa. This suggests that these variants have the same homotetrameric quaternary structure as the wild-type enzyme.

Sulfate dependence of HICA activity

Wild type HICA requires the presence of sulfate ion *in vitro* for maximal activity (2). Unlike α-CA, which is weakly but significantly inhibited by sulfate ion at near molar concentrations (15), HICA is significantly activated by concentrations of sulfate ion up to 400 mM (Figure 1). At higher sulfate concentrations, HICA activity decreases. Like wild-type HICA, the variants V47A and G41A have no detectable CO_2 hydration activity in the absence of sulfate ion.

Activity of HICA-V47A and HICA-G41A

Values of k_{cat}/K_m for both HICA-V47A and HICA-G41A have similar catalytic activity and pH-rate variation as wild-type HICA. At high pH, the k_{cat} values for HICA-V47A is similar to wild-type, but the k_{cat} of HICA-G41A is significantly lower. At pH values below 8.0, catalytic activity of all HICA variants as measured by k_{cat} or k_{cat}/K_m dramatically decreases (Table 2).

Structure of HICA V47A and G41A variants

The overall secondary and tertiary structures of the V47A and G41A variants of HICA are nearly identical to that of wild-type enzyme. The asymmetric unit of the V47A variants in either the orthorhombic or tetragonal crystal forms is composed of a fundamental dimer of HICA representing the probable simplest functional allosteric unit of the enzyme (2). The asymmetric unit of the uncomplexed G41A variant is C2 with dimensions nearly identical to that of wild-type enzyme (2). However, crystals of G41A soaked in 100 mM bicarbonate ion form “double-size” C2 unit cells in which the c-axis is approximately doubled in size. The apparent doubling in size of the unit cell appears to be the result of the binding of a “unique” bicarbonate ion to chains A and C in the protein complex.

Sulfate ion binding

Sulfate ion, which is found in the crystallization medium, is readily identifiable in electron density maps of HICA-V47A and -G41A. In HICA-V47A in the absence of bicarbonate ion (PDB 3E2X), two sulfate ions are bound to a well-recognized anion binding site on the tetramerization interface (2), near the side chains of Arg124 of one chain and Arg160, Lys165, and Arg198 or the neighboring chain. In addition, HICA-V47A also binds two sulfate ions in a hydrophobic pocket near the active site near His98, an anion binding mode previously observed for HICA-Y181F (3). A fifth sulfate ion is bound on the dimerization interface of HICA-V47A between Arg64 from each chain of the fundamental dimer (Figure 2a). The tetragonal form of HICA-V47A (PDB 3E31) does not show clear density for sulfate ion at the tetramerization interface or the hydrophobic pocket near His98. There is some weak electron density on the dimerization interface between adjacent Arg64 residues, but it is not clear if this

NIH-PA Author Manuscript

NIH-PA Author Manuscript

NIH-PA Author Manuscript

is attributable to water or a low-occupancy sulfate ion. In PDB 3E31 it has been modeled as water.

For HICA-G41A in the absence of bicarbonate ion (PDG 3E3G), sulfate ions appear to be bound to the anion binding sites on each of the six tetramerization interfaces. Sulfate ions—4 in all, two on special positions—are also observed bound on the dimerization interface between neighboring Arg64 residues (Figure 2b).

Bicarbonate ion binding

Two distinct binding modes are observed for bicarbonate ion in both HICA variants V47A and G41A. The first of these is a previously observed non-catalytic (allosteric) binding site near Trp39, Arg64, and Tyr181 (2). In HICA-G41A, these include 10 bicarbonate ions bound to chains B (Figure 3a) and D-L. Each of these bicarbonate ions appears to accept hydrogen bonds from Trp39, Arg64, Tyr-181, and two water molecules. The carbonyl oxygen of Val47 appears to accept a hydrogen bond from the −OH of bicarbonate (Figure 3a). This hydrogen bonding network has been observed previously for wild-type HICA complexed with bicarbonate (2). In HICA-V47A (PDB 3E3F), bicarbonate ions occupy analogous sites in both chains in the asymmetric unit, except that Tyr181 is rotated away and does not appear to interact with the bicarbonate ion in this variant (Figure 3b).

The second binding mode of bicarbonate is in a crevice along the dimerization interface near the neighboring pairs of Arg64 and Glu50 side chains, analogous to the sulfate binding sites shown in Figure 2. In HICA-G41A, only one of the 11 bound bicarbonate ions is bound in this mode, in the interface between chains A and C (Figure 3c), the only two chains of this variant that do not have a bicarbonate ion bound in the previously known non-catalytic bicarbonate binding site near Trp39, Arg64, and Tyr181. In HICA-V47A, the two non-catalytic bicarbonate sites and dimerization interface anion binding site in the asymmetric unit are occupied by bicarbonate ions simultaneously (Figure 3b). The binding of the bicarbonate ion in the dimerization site is the same for both the V47A and G41A variants. The bicarbonate ion appears to accept hydrogen bonds from both Arg64 residues on the dimer interface. One Glu50 side chain appears to accept a hydrogen bond from the −OH group of bicarbonate; the other Glu apparently accepts a hydrogen bond from water, which also donates a hydrogen bond to the bicarbonate ion.

It is noted for completeness that HICA-V47A (PDB 3E3F) harbors a fourth bicarbonate ion bound to the tetramerization interface where anions such as sulfate (2) or phosphate (3) have been previously observed to bind.

Discussion

The HICA variants V47A and G41A were expressly constructed to critically test the effect of steric crowding in the non-catalytic, allosteric bicarbonate binding site of HICA. One might have expected HICA-V47A to have lost the steric coupling mechanism required to expel bicarbonate ion from the T-state and stabilize the R-state, leading to an enzyme with reduced activity. Yet, HICA-V47A has a k_{cat} and k_{cat}/K_m for CO_2 hydration that is comparable to wild-type enzyme, and still shows a dramatic decrease in k_{cat} and k_{cat}/K_m at pH values below 8.0 that is typical of type II β-CAs (1). One might expect that HICA-G41A would be incapable of binding allosteric bicarbonate because of the steric interference of the methyl side chain of Ala41 in this variant, leading to an enzyme with enhanced activity, especially at low *p*H where the inactive T-state is thought to predominate (2,3); yet, HICA-G41A has k_{cat}/K_m values for CO_2 hydration similar to wild-type enzyme, and its k_{cat} at high pH is actually significantly *lower* than wild-type. Why mutation of Gly41 would have such a significant effect on k_{cat} is not obvious from either a mechanistic or structural viewpoint. In addition, it is clear from the

NIH-PA Author Manuscript

NIH-PA Author Manuscript

NIH-PA Author Manuscript

crystallographic data (Figure 3a) that bicarbonate ion can still bind in the non-catalytic, allosteric site. Apparently, the β-sheet containing the variant Ala41 residue and/or the bicarbonate ion have subtly shifted sufficiently to be able to accommodate both the methyl side chain of Ala41 and bicarbonate ion in the allosteric binding site. So it would appear that the catalytic activity of the enzyme and the function of the allosteric bicarbonate binding site are not so easily disrupted by single side chain alterations at Val47 or Gly41.

Evidence for a bicarbonate "escort" site

Unexpectedly, the HICA variants V47A and G41A in the presence of bicarbonate ion have revealed a highly probable intermediate bicarbonate binding site on the dimerization interface of the enzyme near a pair of Arg64 and Glu50 residues (Figures 3b and 3c). Bicarbonate binding to this site has been observed previously for the allosteric site variant Y181F (3), as well as here for one of the dimerization interfaces of 12 protein chains in the asymmetric unit of the variant G41A (Figure 3c), and for the variant V47A (Figure 3b). The observation of this bicarbonate binding site in multiple crystal structures suggests that it is not artifactual, and may be functionally relevant. The location of this bicarbonate binding in close proximity to the allosteric bicarbonate binding site strongly suggests that it represents an intermediate along the ingress/egress route for allosteric bicarbonate. We propose designating this bicarbonate binding site the "escort" site, a jumping-off point for bicarbonate ions transitioning between bulk solution and the allosteric binding site of HICA. Because the structure of the wild-type enzyme and the variants described here are identical overall and in the "escort" site region, it seems likely that bicarbonate ions can bind to this site in the wild-type enzyme as well, although anion binding to the "escort" site region in wild-type enzyme has not been observed crystallographically (2). The crystal structure HICA-V47A complexed with bicarbonate ion suggests that the allosteric and "escort" binding sites are not mutually exclusive, but can be occupied simultaneously (Figure 3b). It seems remarkable that it is possible to "catch" the binding of bicarbonate ion in the "escort" site but not the allosteric site in HICA-Y181F (3) and chains A and C only for HICA-G41A (Figure 3c), while both the "escort" and allosteric sites are both occupied in HICA-V47A (Figure 3b). One can only assume that variations in intermolecular contacts and solvent channels in the various crystal forms and variants of HICA are responsible for the lucky happenstance of observing bicarbonate binding at the "escort" site.

Examination of the HICA-V47A structure (PDB 3E3F) with CAVER (16,17) reveals plausible entry/exit routes for allosteric bicarbonate ion (Figure 4). One of these routes (colored orange) passes down the dimerization interface, past opposing Glu50 and Arg64 residues in this crevice and into the allosteric site. Another route (colored pink) enters/exits just to the side of the dimerization interface, between Arg46, Ala47, and Leu52. This route appears to be possible in HICA-V47A only because Tyr181 has rotated away from the allosteric site, and is not engaged in a hydrogen bonding interaction with allosteric bicarbonate ion. In wild-type HICA (2) and the G41A variant (Figure 3a), Tyr 181 is engaged in a hydrogen bonding interaction with both the allosteric bicarbonate ion and the main-chain amide nitrogen of Val47 and/or the "unique" water (1,2). At first glance, the intermolecular contacts in the bicarbonate "escort" site look odd. While it is certainly chemically reasonable to expect that bicarbonate ion would interact with the pair of Arg64 residues in this site, the presumably negatively charged pair of Glu50 residues looks less inviting because of the potential charge repulsion involved. Nevertheless, the data suggest that one Glu residue—Glu50A in HICA-V47A (Figure 3b) and Glu50C in HICA-G41A (Figure 3c)—is within direct hydrogen bonding distance of one of the bicarbonate oxygen atoms, presumably the −OH oxygen. The other Glu residue—Glu50B in HICA-V47A (Figure 3b) and Glu50A in HICA-G41A (Figure 3c)—appears to interact with bicarbonate ion through a water molecule which likely donates hydrogen bonds to both Glu50 and bicarbonate ion.

NIH-PA Author Manuscript

NIH-PA Author Manuscript

NIH-PA Author Manuscript

Precedent for the interaction of carboxylates with protein-bound bicarbonate ion comes from unlikely sources: cyclopropane fatty acid synthase from *E. coli* (18) and the mycolic acid cyclopropane synthases from *Mycobacterium tuberculosis* (19), in which bicarbonate ion is thought to be a catalytically essential cofactor. In these synthases, the bound bicarbonate ion interacts with three hydrogen bond donors: a Tyr, His and a backbone amide. A single Glu side chain interacts directly with the bicarbonate ion presumably as a hydrogen bond acceptor (supporting information, Figure S1). This is analogous to HICA, in which two Arg residues and one water molecule act as hydrogen bond donors, and Glu side chain acts as a hydrogen bond acceptor with bicarbonate ion. Although Courtois and Ploux (18) speculated that the His residue of *E. coli* cyclopropane fatty acid synthase was neutral, it seems more likely that this residue is protonated to help neutralize negative charge in the binding site, analogous to the Arg residues in HICA.

Activation of HICA by sulfate ion

The existence of a bicarbonate "escort" site in HICA offers a possible explanation for the observed activation of HICA by sulfate ion *in vitro*. This phenomenon has been well-known since the initial kinetic studies of HICA (2), but has never had a satisfactory explanation. A number of X-ray crystallographic structures of HICA and its variants, including Y181F (PDB 3E28, Figure 5) (3) and variants G41A (Figure 3b) and V47A (Figure 3a), bind sulfate ion at the bicarbonate "escort" site in the absence of bicarbonate ion. Thus, it seems likely that sulfate ion acts as a competitive inhibitor for bicarbonate ion at the "escort" site, hindering access of bicarbonate ion to produce the inactive, T-state of the enzyme. In the absence of sulfate ion *in vitro*, very little or no CO_2 hydration activity can be observed for HICA, most likely due to the accumulation of the product, HCO_3^-, which quickly converts the enzyme to the T-state. The presence of sulfate ion at the "escort" site would prevent the ingress of bicarbonate ion to the allosteric site, largely preserving enzyme activity during the data collection period for CO_2 hydration, which is typically100-1000 ms for stopped-flow spectrophotometry. One might reasonably expect non-Michaelis-Menten kinetics in such a complex system in which sulfate and product (bicarbonate) are competing for the escort site. However, no significant deviation from apparent Michaelis-Menten kinetics was observed for either wild-type enzyme or the variants G41A or V47A during the time span of stopped-flow measurements. A likely explanation is that the reorganization of the enzyme from the active, R-state, to the inactive, T-state is very likely to require a time scale significantly longer than that required for stopped-flow kinetics, perhaps in the seconds to tens of seconds.

It does not seem likely that the binding of sulfate to HICA is physiologically relevant, as the sulfate concentrations required for maximum effect (200-400 mM) are much higher than intracellular concentrations of sulfate ion. However, it is possible that other anions could also bind to the "escort" site. The HICA variant W39F, which was crystallized from low concentrations (40-80 mM) of ammonium phosphate (PDB 3E24), was found to have phosphate ion bound to the bicarbonate "escort" site (3). It is tempting to speculate that physiological concentrations (mM levels) of phosphate ion could act as an indirect allosteric effector of HICA by hindering the ability of bicarbonate ion shift the allosteric equilibrium of HICA toward the T-state *in vivo*.

Conclusion

The HICA variants V47A and G41A are similar to wild-type HICA in overall structure and catalytic ability toward CO_2 hydration. Despite these variants having significantly different sterics in the allosteric binding site for bicarbonate compared to HICA, crystals of these protein variants prepared in the presence of bicarbonate ion are found to have bicarbonate present in the allosteric site. In addition, these variants exhibit an additional bicarbonate binding site on

NIH-PA Author Manuscript

NIH-PA Author Manuscript

NIH-PA Author Manuscript

the dimerization interface—a bicarbonate "escort" site—that is likely to be an intermediate binding site along the ingress/egress route for allosteric bicarbonate. The kinetic and structural evidence reported here suggest that sulfate, and perhaps other anions, can bind to the "escort" site and prevent the binding of bicarbonate ion to the allosteric site, thereby "activating" the enzyme by stabilizing the active R-state relative to the inactive T-state of the enzyme.

Supplementary Material

Refer to Web version on PubMed Central for supplementary material.

References

1. Rowlett RS. Structure and catalytic mechanism of the β-carbonic anhydrases. Biochimica et Biophysica Acta (BBA) - Proteins & Proteomics 2010;1804:362–373.
2. Cronk JD, Rowlett RS, Zhang KYJ, Tu C, Endrizzi JA, Lee J, Gareiss PC, Preiss JR. Identification of a Novel Noncatalytic Bicarbonate Binding Site in Eubacterial beta-Carbonic Anhydrase. Biochemistry 2006;45:4351–4361. [PubMed: 16584170]
3. Rowlett RS, Tu C, Lee J, Herman AG, Chapnick DA, Shah SH, Gareiss PC. Allosteric Site Variants of Haemophilus influenzae beta-Carbonic Anhydrase. Biochemistry 2009;48:6146–6156. [PubMed: 19459702]
4. Sarkar G, Sommer SS. The Megaprimer Method of Site-Directed Mutagenesis. BioTechniques 1990;8:404–407. [PubMed: 2340178]
5. Khalifah RG. Carbon dioxide hydration activity of carbonic anhydrase. I. Stop-flow kinetic studies on the native human isoenzymes B and C. J Biol Chem 1971;246:2561–2573. [PubMed: 4994926]
6. Pocker Y, Bjorkquist DW. Comparative studies of bovine carbonic anhydrase in water and water-d2. Stopped-flow studies of the kinetics of interconversion of carbon dioxide and bicarbonate(1-) ion. Biochemistry 1977;16:5698–5707. [PubMed: 22343]
7. Ghannam AF, Tsen W, Rowlett RS. Activation parameters for the carbonic anhydrase II-catalyzed hydration of carbon dioxide. J Biol Chem 1986;261:1164–1169. [PubMed: 3080418]
8. Rowlett RS, Gargiulo NJ III, Santoli FA, Jackson JM, Corbett AH. Activation and inhibition of bovine carbonic anhydrase III by dianions. J Biol Chem 1991;266:933–941. [PubMed: 1898739]
9. Leslie AGW. Recent changes to the MOSFLM package for processing film and image data. Joint CCP4 and ESF-EACMB Newsletter on Protein Crystallography. 1992
10. CCP4 (Collaborative Computational Project, N. The CCP4 Suite: Programs for protein crystallography. Acta Crystallographica Section D- Biological Crystallography 1994;50:760–763.
11. McCoy AJ, Grosse-Kunstleve RW, Adams PD, Winn MD, Storoni LC, Read RJ. Phaser crystallographic software. J Appl Crystallogr 2007;40:658–674. [PubMed: 19461840]
12. Murshudov GN, Vagin AA, Dodson EJ. Refinement of macromolecular structures by the maximum-likelihood method. Acta Crystallographica Section D-Biological Crystallography 1997;53:240–255.
13. Emsley P, Cowtan K. Coot: model-building tools for molecular graphics. Acta Crystallogr D 2004;60:2126–2132. [PubMed: 15572765]
14. Winn MD, Isupov MN, Murshudov GN. Use of TLS parameters to model anisotropic displacements in macromolecular refinement. Acta Crystallographica Section D-Biological Crystallography 2001;57:122–133.
15. Innocenti A, Vullo D, Scozzafava A, Supuran CT. Carbonic anhydrase inhibitors. Inhibition of isozymes I, II, IV, V, and IX with anions isosteric and isoelectronic with sulfate, nitrate, and carbonate. Bioorg Med Chem Lett 2005;15:567–571. [PubMed: 15664814]
16. Petrek M, Otyepka M, Banas P, Kosinova P, Koca J, Damborsky J. CAVER: a new tool to explore routes from protein clefts, pockets and cavities. Bmc Bioinformatics 2006;7
17. Damborsky J, Petrek M, Banas P, Otyepka M. Identification of tunnels in proteins, nucleic acids, inorganic materials and molecular ensembles. Biotechnology Journal 2007;2:62–67. [PubMed: 17183511]
18. Courtois F, Ploux O. Escherichia coli cyclopropane fatty acid synthase: Is a bound bicarbonate ion the active-site base? Biochemistry 2005;44:13583–13590. [PubMed: 16216082]

NIH-PA Author Manuscript

NIH-PA Author Manuscript

NIH-PA Author Manuscript

19. Huang CC, Smith CV, Glickman MS, Jacobs WR, Sacchettini JC. Crystal structures of mycolic acid cyclopropane synthases from Mycobacterium tuberculosis. Journal of Biological Chemistry 2002;277:11559–11569. [PubMed: 11756461]

20. Engh RA, Huber R. Accurate bond and angle parameters for X-ray protein structure refinement. Acta Crystallographica Section A 1991;47:392–400.

21. DeLano, WL. The PyMOL Molecular Graphics System. DeLano Scientific; San Carlos, CA, USA: 2002.

NIH-PA Author Manuscript

NIH-PA Author Manuscript

NIH-PA Author Manuscript

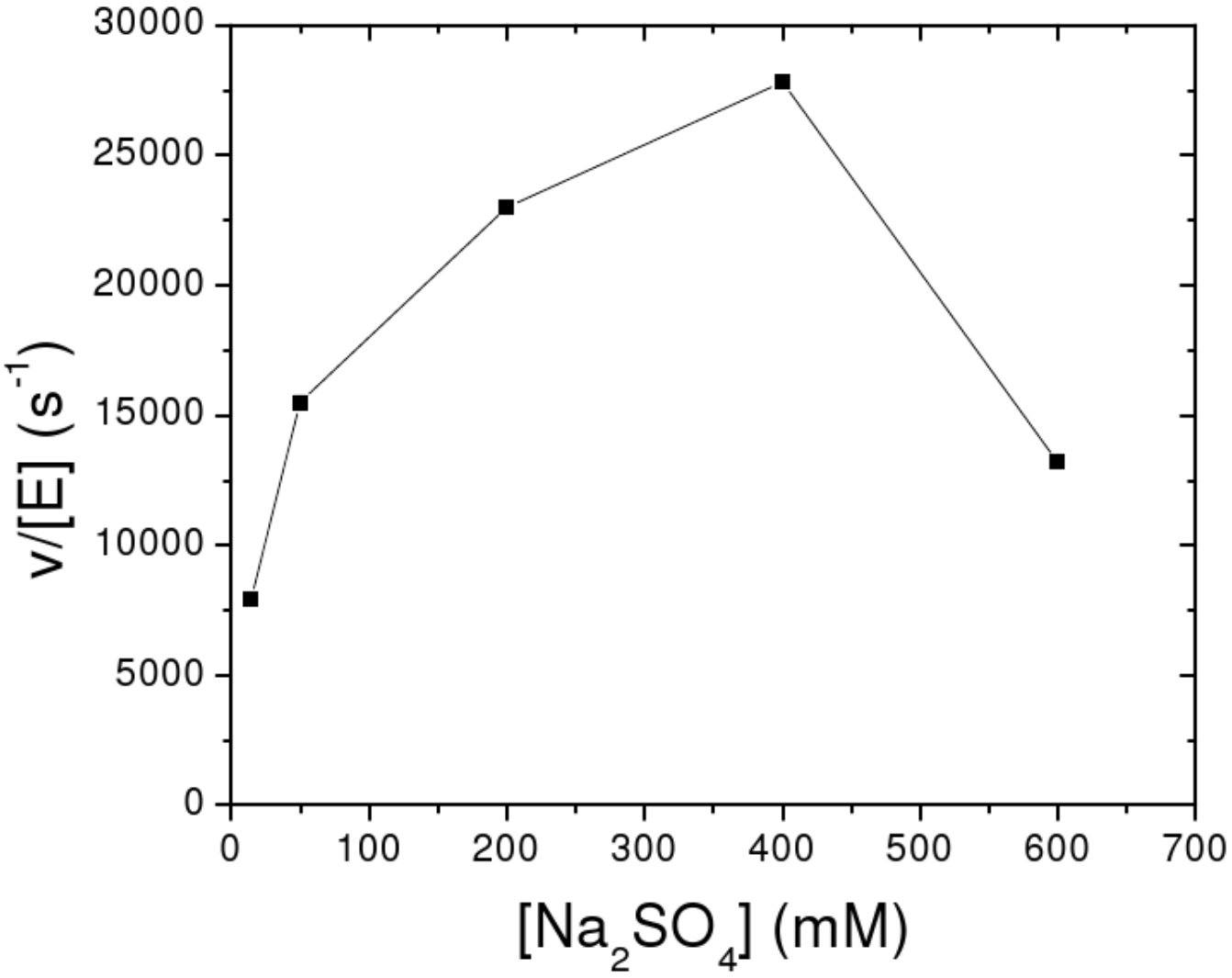

Figure 1.
Sulfate dependence of CO_2 hydration activity of wild-type HICA. Reaction conditions were 40 mM bicine pH 8.50, 1 μ*M* EDTA, 8.0 mM CO_2, 25 °C.

NIH-PA Author Manuscript
NIH-PA Author Manuscript
NIH-PA Author Manuscript

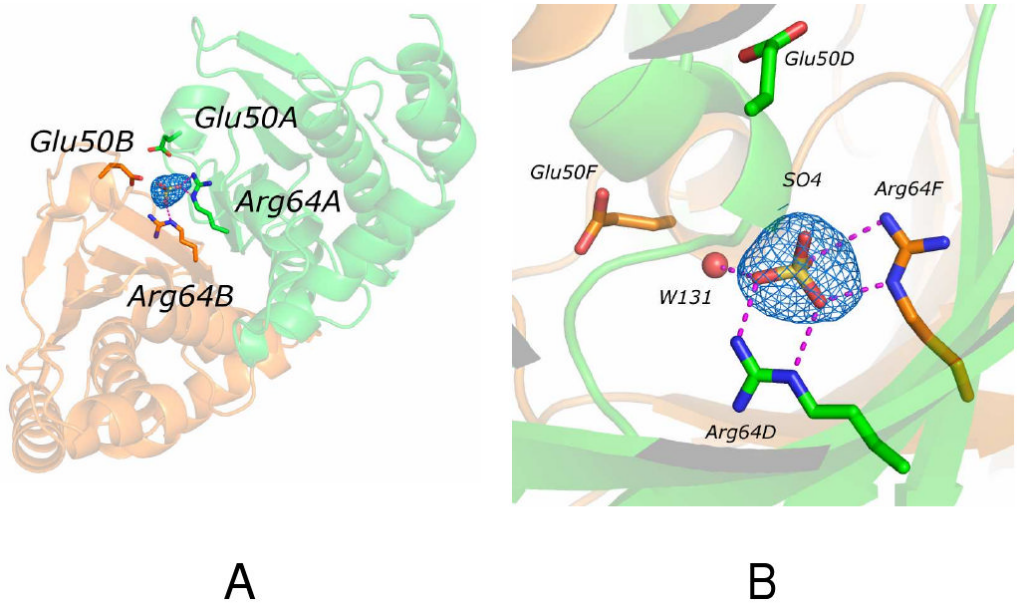

Figure 2.

Sulfate binding to the dimerization interface of HICA. (A) F_o-F_c omit map of sulfate binding to HICA-V47A, contoured at 3.0 σ. Fundamental dimer is depicted: green, chain A; orange, chain B. Tetramerization interface is at lower right. (B) F_o-F_c omit map of sulfate binding to HICA-G41A, contoured at 2.0 σ. Chain D; green; Chain F, orange. Figures created with Pymol (21). For all figures, magenta dashes indicate atoms within hydrogen bonding distance (<3.5 Å).

NIH-PA Author Manuscript

NIH-PA Author Manuscript

NIH-PA Author Manuscript

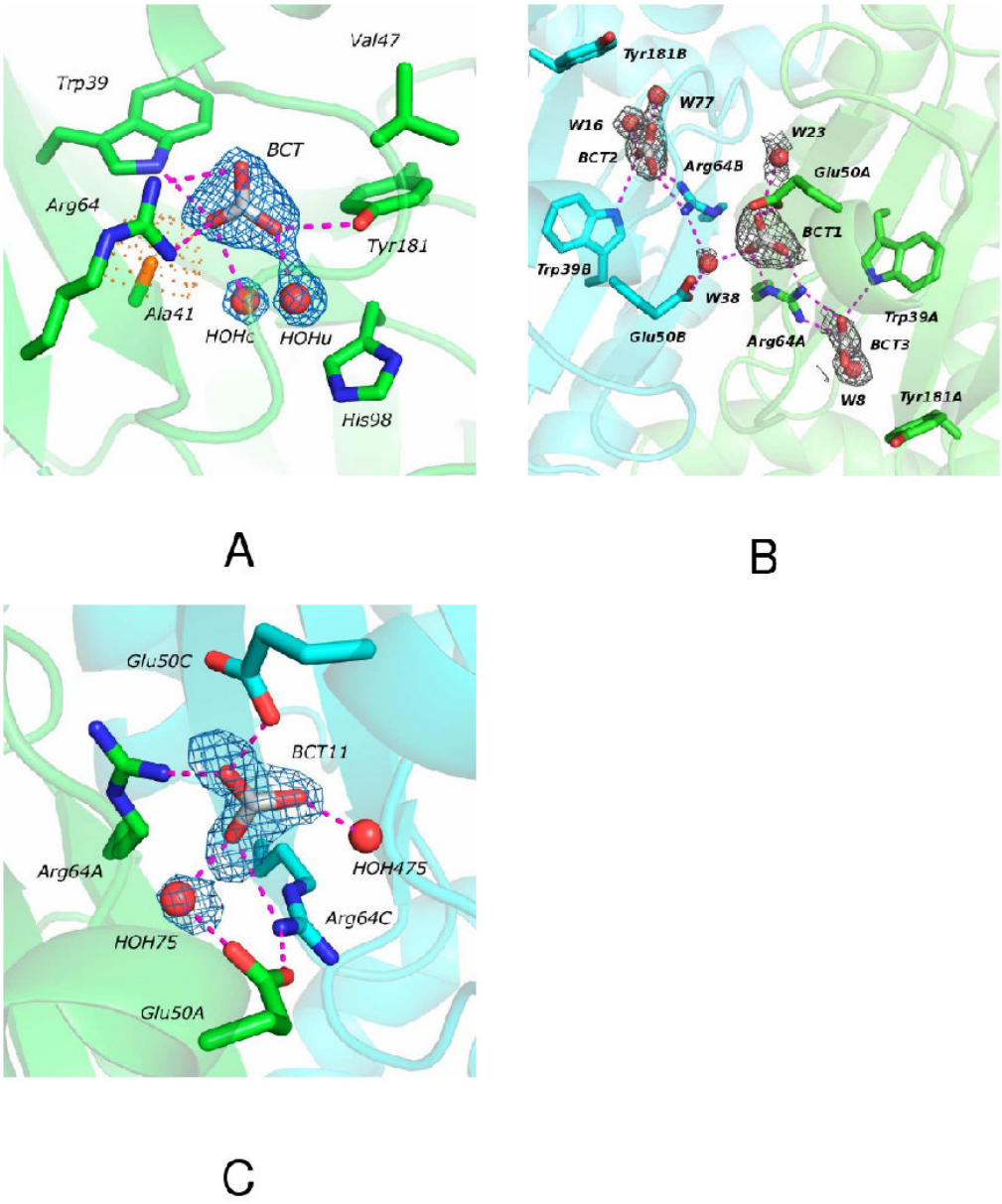

Figure 3.

Bicarbonate binding to HICA variants. (A) F_o-F_c omit map of bicarbonate binding to the allosteric site of HICA-G41A in chain B, contoured at 3.0 σ. HOHc and HOHu represent the "common" and "unique" water molecules in the binding site (1,2). The C_β of Ala41 is colored orange; orange dots indicate the van der Waals radius of the C_β of Ala41(B) F_o-F_c omit map of bicarbonate binding to the allosteric (BCT2 & BCT3) and "escort" (BCT1) sites of HICA-V47A, contoured at 1.5 σ. Green, chain A, cyan, chain B. (C) F_o-F_c omit map of bicarbonate binding to the "escort" site of HICA-G41A, contoured at 3.0 σ. Green, chain A, cyan, chain C. Figures created with Pymol (21). For all figures, magenta dashes indicate atoms within hydrogen bonding distance (<3.5 Å).

NIH-PA Author Manuscript
NIH-PA Author Manuscript
NIH-PA Author Manuscript

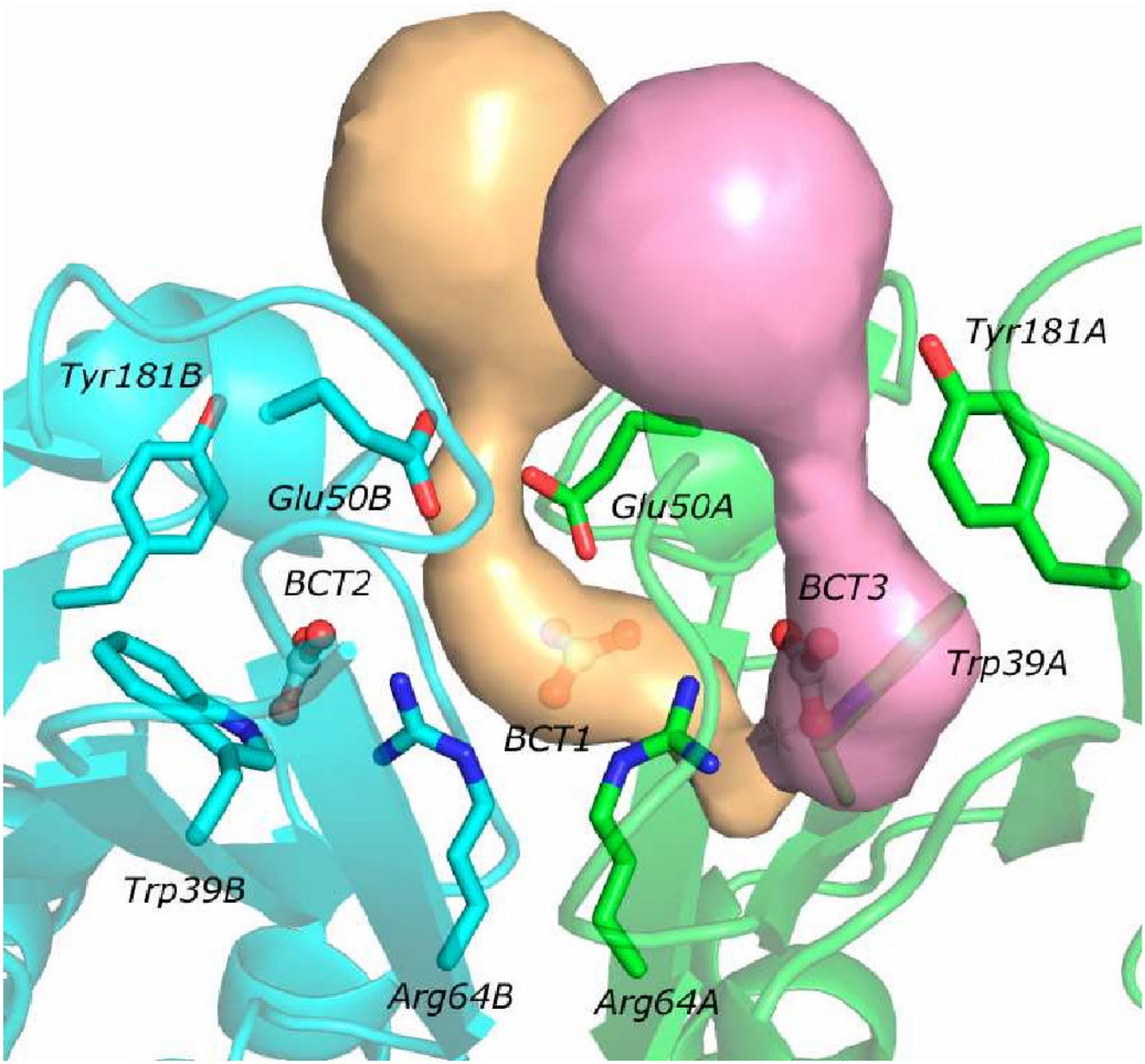

Figure 4.

Depiction of tunnels leading to the allosteric bicarbonate binding site in chain A of HICA-V47A (PDB 3E3F). Key residues in the allosteric and "escort" sites are depicted as sticks. Chain A is colored green; chain B is colored cyan. Bicarbonate ions BCT2 and BCT3 are bound to the allosteric sites; BCT 1 is bound to the "escort" site. Tunnels are depicted as colored surfaces leading to the BCT3 allosteric site. The orange-colored tunnel passes through the "escort" site. The pink-colored tunnel passes by Tyr181, which is rotated away from the allosteric site in this HICA variant. Figure created with Pymol (21). Tunnels were computed using CAVER 2.0 (16,17).

NIH-PA Author Manuscript
NIH-PA Author Manuscript
NIH-PA Author Manuscript

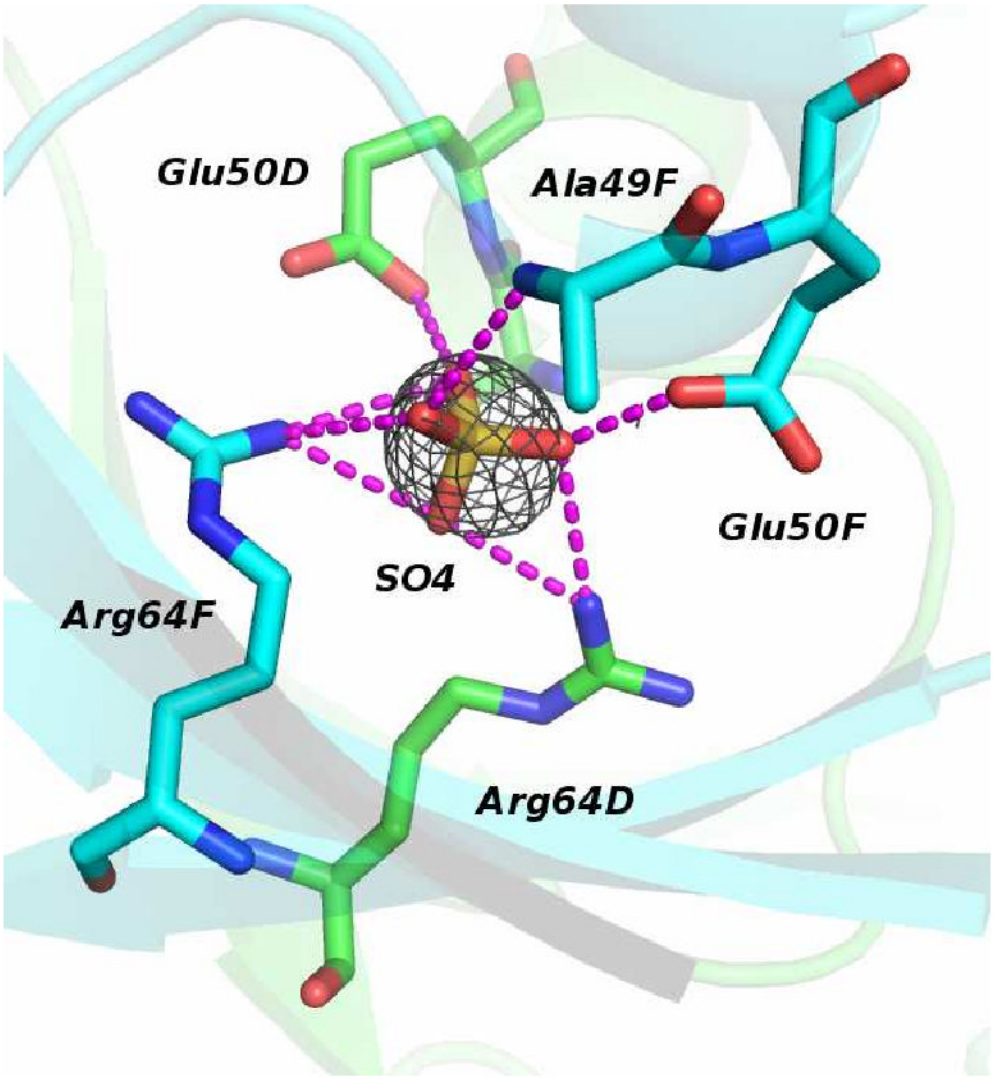

Figure 5.
F_o-F_c omit map of sulfate binding to the "escort" site in HICA-Y181F (PDB 3E28) (3), contoured at 2.0 σ. Chain D, green; Chain F, cyan. Figures created with Pymol (21). Magenta dashes indicate atoms within hydrogen bonding distance (<3.5 Å).

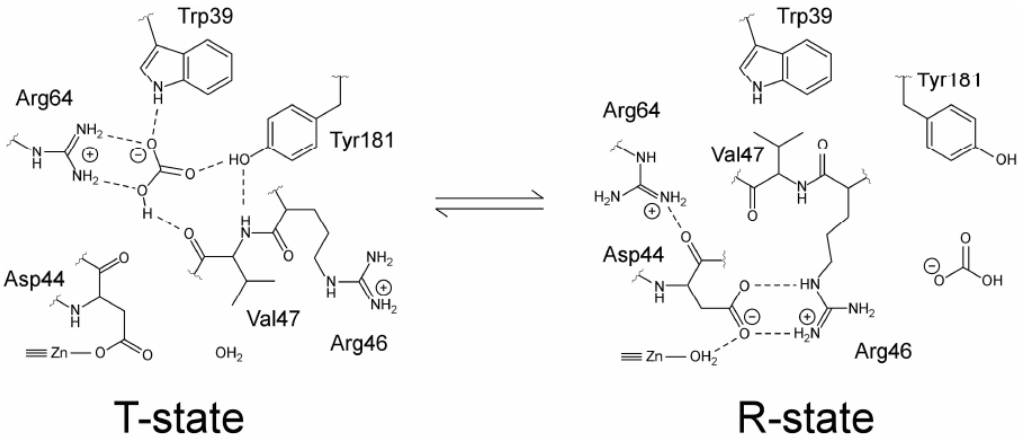

Scheme 1.

Structural schematic of key active site and noncatalytic bicarbonate binding site interactions in the hypothesized active (R-state) and inactive (T-state) conformations of HICA (2).

NIH-PA Author Manuscript NIH-PA Author Manuscript NIH-PA Author Manuscript

NIH-PA Author Manuscript NIH-PA Author Manuscript NIH-PA Author Manuscript

Table 1

Data collection and refinement statistics for HICA variants[a]

	G41A (PDB 3E3G)	G41A + 100 mM HCO_3^- (PDB 3E3I)	V47A (PDB 3E2X)	V47A (PDB 3E31)	V47A + 100 mM HCO_3^- (PDB 3E3F)
			Data collection statistics		
Source	CHESS beamline F2	CHESS beamline F2	CHESS beamline F2	CHESS beamline F2	CHESS beamline F2
Wavelength (Å)	0.97	0.98	0.97	0.97	0.98
Space Group	C2	C2	$I2_12_12_1$	$P4_12_12$	$P4_12_12$
Cell parameters (Å)	231.9, 145.2, 53.0	229.6, 144.4, 104.9	48.1, 133.3, 143.9	82.3, 82.3, 188.8	83.9, 83.9, 184.9
(°)	90, 93.8, 90	90, 94.4, 90	90, 90, 90	90, 90, 90	90, 90, 90
Resolution (Å)	39.4−2.30 (2.36-2.30)	29.8−2.00 (2.05-2.00)	34.0−2.55 (2.62-2.55)	37.7−2.95 (3.11-2.95)	28.9−2.30 (2.42-2.30)
Unique reflections	79059	205440	14811	14391	30001
Redundancy	6.9 (4.6)	4.8 (3.1)	4.0 (3.2)	16.8 (5.8)	8.2 (4.0)
Completeness	98.1 (88.2)	89.6 (55.6)	95.7 (82.0)	99.9 (100)	99.2 (94.6)
R_{sym} (%)	0.088 (0.516)	0.055 (0.475)	0.094 (0.482)	0.082(0.493)	0.066 (0.367)
$\langle I \rangle / \langle \sigma I \rangle$ [b]	19.1 (2.0)	19.1 (1.9)	13.8 (1.6)	34.2 (5.8)	22.6 (2.1)
			Refinement statistics		
Reflections in test set	3804	10347	743	718	1523
R_{work} (%)	0.197	0.201	0.211	0.197	0.193
R_{free} (%)	0.234	0.236	0.283	0.247	0.230
No. of atoms					
Protein	9959	20350	2920	2887	2894
Ligand	85	109	25	0	25
Ion	6	12	2	2	2
Solvent	133	604	0	16	84
rmsd from ideal[c]					
Bond distance (Å)	0.011	0.011	0.013	0.016	0.017
Bond angle (°)	1.2	1.2	1.4	1.6	1.6
Ramachandran plot outliers (%)[d]	2.8	2.4	7.1	5.8	1.9

NIH-PA Author Manuscript
NIH-PA Author Manuscript
NIH-PA Author Manuscript

[a] Values in parentheses represent data for the highest resolution shell.

[b] Reported as ‹‹I›/σ‹I›› in SCALA or SCALEPACK.

[c] Ideal values from Engh and Huber (20).

[d] Calculated using a strict boundary Ramachandran plot (13).

Biochemistry. Author manuscript; available in PMC 2011 May 4.

NIH-PA Author Manuscript

NIH-PA Author Manuscript

NIH-PA Author Manuscript

Table 2

Catalytic rate constants for CO_2 hydration catalyzed by wild-type, G41A, and V47A variants of HICA[a]

Enzyme	pH 7.50		pH 9.0	
	k_{cat} (ms^{-1})	k_{cat}/K_m ($\mu M^{-1}\ s^{-1}$)	k_{cat} (ms^{-1})	k_{cat}/K_m ($\mu M^{-1}\ s^{-1}$)
wild type (2)	2.4	0.24	64	5.6
G41A	1.10 ± 0.07	0.42 ± 0.07	5.0 ± 0.3	7.0 ± 1.7
V47A	5.3 ± 0.2	0.88 ± 0.04	140 ± 20	7.0 ± 2.6

[a]Reaction conditions were 25 °C, 40 mM 1,2-dimethylimidazole (pH 9.0) or 1-methylimizazole (pH 7.50), 1 μ*M* EDTA, 250 mM Na_2SO_4.